Subsurface Structure Detection Using Geomagnetic Data Approach in Wadi Araba area, Gulf of Suez, Egypt

Abdelbaset M. Abudeif [*], Mahmoud Abdallah Ali, Mohammed A. Mohammed

Geology Department, Faculty of Science, Sohag University, Sohag, 82524, Egypt.
[*]*E-mail:* a.abudeif@science.sohag.edu.eg

Abstract: One of the most attractive locations for oil and natural gas extraction is the Wadi Araba region in the Gulf of Suez, Egypt. The main objective of the present investigation is the analysis and interpretation of the available aeromagnetic data utilizing various modern processing techniques to map the subsurface structural framework and estimate the depth of these structures in the Wadi Araba. The total magnetic intensity (TMI) anomaly map of the study area was reduced to the north magnetic pole (RTP). This map was separated into regional and residual maps, then, they were analyzed qualitatively and quantitatively by Geosoft Oasis Montaj Software. Results of trend analysis indicated that there are four major trends in the study area, NW-SE (Suez Rift), NE-SE (Syrian Arc), E-W (Tethyan), and N-S (East African) arranged in decreasing order of their frequency magnitude where the trends of Suez and the Syrian are the most common. The deduced orientations are agreeable and presented in the surface structures. The presence of such two major trends (NW-SE) and (NE-SW) increases the potential of the study area to contain petroleum traps. This study deduced that the depth to the basement complex varies from 0.5 to 3 Km with an average of 1.8 Km, as indicated by the result of 2D power spectrum and 3D Euler deconvolution. The trend analysis indicates that the area is dissected by a group of structural fault trends that may be implemented as structural traps for petroleum accumulation in this region which needs more seismic studies to explore their types and geometry.

Keywords: Aeromagnetic data; subsurface trends; regionals; residuals; Euler deconvolution effect.

1. Introduction

Source depths and variations in magnetic susceptibilities are associated with magnetic data. As a result, these data are employed to identify the positions, depths, forms, and trends of the magnetic objects that they have produced. Due to the increased use of magnetic data for reconnaissance investigations of mineral and petroleum accumulations, this goal has recently assumed significance. To determine whether there are petroleum traps in the study area, we utilized the criteria that were available to define the subsurface structures in the area.

The main aim of this work is to define the tectonic structure of the studied area, identify any potential hydrocarbon traps, and determine the thickness of the sedimentary cover of the underlying basement rock.

The study area is located in the Eastern Desert of Egypt, on the northern section of the Gulf of Suez, and is roughly 605.87 km² in size (Fig. **1**). It is delimited by latitudes 29°00′00″N and 29°10′00″N and longitudes 32°20′00″E and 32°40′00″E. The study region is an important part of Wadi Araba, which is bordered to the north and south by the Galala Plateaus, to the east by the Gulf of Suez, and to the west by the Eastern Desert's central limestone plateau. According to [47] horizontal compression is thought to be the cause of Egypt's structural pattern in general and that of the Gulf of Suez region in particular. Bouguer gravity maps were utilized by [30, 37] to investigate the structural framework of the Gulf of Suez region.

Numerous authors have proposed the existence of the block-faulting phenomenon in Egypt's Eastern Desert [21, 45, 26, 23].

[28, 31] considered the structure of Wadi Araba as a regional plunging anticline, trending NE and covered by a multitude of normal faults. The northern Galala/Wadi Araba High (NGWA High) is separated by east–northeast trending faults that run perpendicular to the younger Gulf of Suez faults, which resulted from the Miocene opening of the Gulf [9].

The Syrian arc system is shown to have a NE-SW orientation because the studied area is one of its most significant components. Additionally, the NW-SE trend of the Gulf of Suez opening must have an impact on the study region. In the studied area, there are both N-S and E-W orientations. The Syrian Arc can be traced from Syria to the central Western Desert of Egypt, via Sinai and the northern part of the Eastern Desert. It is composed of the Palmyride and Sinai-Negev fold belts, both having similar lithologic and structural characteristics [43].

The studied area is more likely to develop petroleum traps due to the complexity of the structural patterns. Regional structures in the northern Desert have a strong influence on the complexity of the local structure.

2. Geological setting

The Wadi Araba volcanics were extruded into the crest of the Wadi Araba anticline. The axis and plunge of which trends from East to West. These alkali basaltic rocks appear to belong to an active continental margin environment, being extruded within uplifted areas [5]. There is no evidence that the ascending lava was interbedded within the country rocks in the form of sills
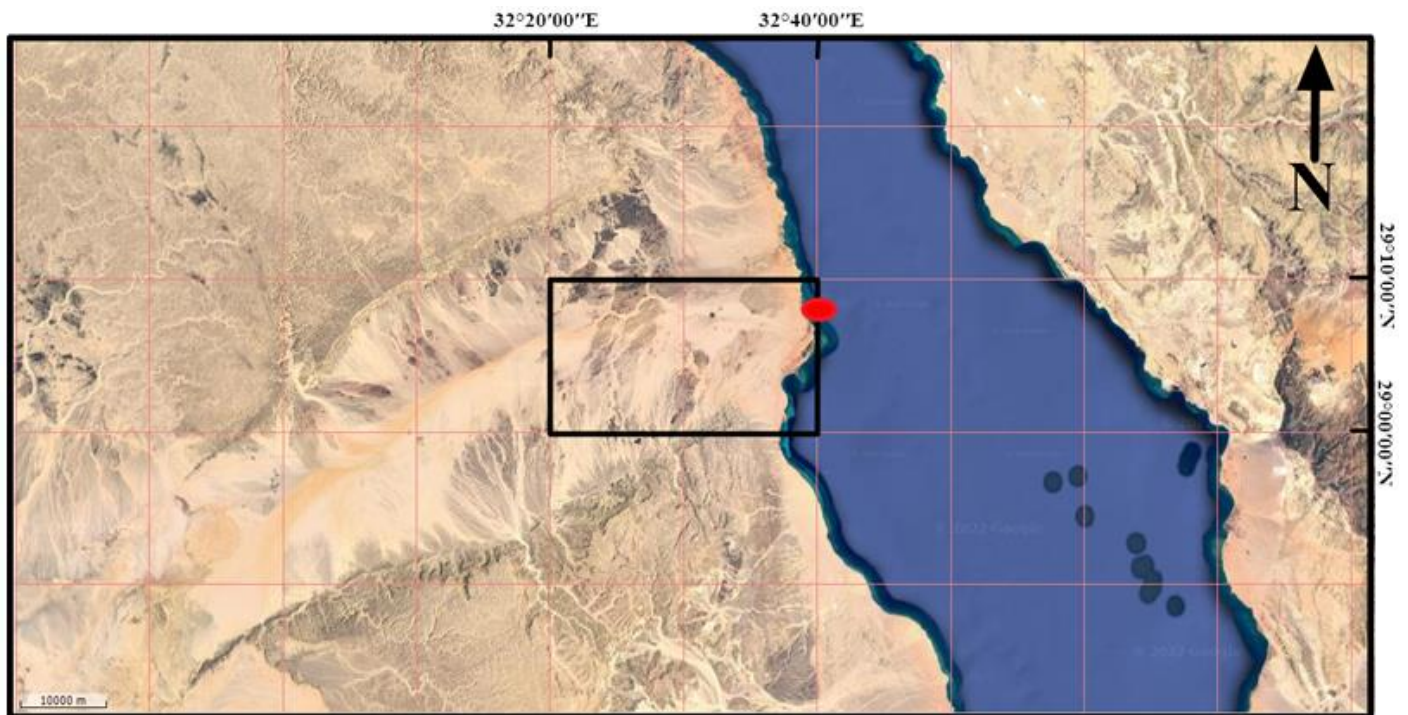
Fig. 1: Location map of the study area; the black box delineates the study area; the red circle refers to the EWA-1X well.

or sheets. The volcanicity obviously did not affect the penetrated sedimentary rocks very much. However, there is a clear relationship between the occurrences of these basaltic plugs and dykes, and the faults occurring in the area [4].

The volcanic rocks of Wadi Araba and Abu Darag, the western side of the Gulf of Suez, are considered as related to the phase of Early Cretaceous Volcanicity. However, a slightly younger volcanic pulse may have followed. The rocks occur mainly as dikes and plugs cutting essentially the Upper Paleozoic sedimentary series which are exposed at the core of Wadi Araba structure and in several localities in Abu Darag area [4]. Volcanic plugs are found more dominantly than dykes in Wadi Araba area. [4] established a linear relation of these plugs with the structural features, thus suggesting that they were brought about along the main fault and fracture planes in positions where these planes intersect other concealed deep faults or fractures. The linear arrangement of the eruptions recorded is more or less parallel to the nearly E-W axis of Wadi Araba structure. Some dykes have other subordinate trends coinciding with the fault directions. Several lithostratigraphic units, extending from the Late Paleozoic to the Quaternary, comprise the visible geological units in the studied area. These units can be summarized from (**Figs 2, 3** and **4**).

2.1. Rod El-Hamal Formation

The Rod El-Hamal Formation was first recognized as Carboniferous in age by [2] at its particular locality in the scarp of the northern Galala Plateau, Wadi Araba area, west side of

Gulf of Suez at the intersection of Wadi Araba and Wadi Rod El- Hamal, where it is best visible.

2.2. Qiseib Formation

This Formation is Permo-Triassic in age and is primarily made up of variably colored, bleached, and heavily bedded sandstone [18].

2.3. Jurassic sediments

Sandstones, mails, shales, and limestones compose the greatest visible thickness of the Jurassic layers, which are also

visible on the NW shore of the Gulf of Suez [38].

2.4. Malha Formation

The Nubian sandstone and shales formation correspond to this formation. It shows the Early Cretaceous outcropping deposits in the western Gulf of Suez area [3].

2.5. Galala Formation

During the Cenomanian, the Neotethyan Ocean's southern shoreline was where the southern Galala Plateau was located. The layering of marine sediments over non-marine sandstones from the Malha Formation at the foot of the Galala Formation provides evidence of a marine transgression [46].

2.6. Maghra El Hadida Formation

The southern Galala Plateau in Wadi Araba contains the Cenomanian-Turonian (Upper Cretaceous) Galala and Maghra el Hadida formations, which show how marine depositional systems responded to the early Late Cretaceous transgression [46].

2.7. Duwi Formation

The phosphate-bearing layers of Wadi Araba are part of this formation [19].

2.8. Sudr Formation

This formation, which is composed of chalky limestone, dates back to the Late Cretaceous and rests unconformably over the Duwi Formation [40].

2.9. Wadi Irkas Formation

This formation's deposits are mostly made up of sandy limestone and well-bedded sandstone [20].

2.10. Mokattam Formation

This formation is of Middle Eocene age and mostly consists of hard, largely bedded limestone at the top horizon and crystalline limestone at the lower level [39].

Most of the Wadi Araba area is covered by these sediments, which are primarily made up of clastic sediments with a variety of textures. The primary courses of the wadis contain wadi sediments, which are distinct gravel, silt, and sand particles [18].

2.11 Quaternary Sediments

GEBEL EL ZEIT PETROLUM Co.

PETROZEIT

COMPOSITE WELL LOG

Well Name		EWA-1X (EAST WADI ARABA-1X)	
Lat.	29°08'45.927"N	Driller TD.	5000 ft (1524m)
Long.	32°40'46.002"E	E-Log TD.	5003ft
Rig Type	Offshore	Formation at TD.	Nubian Sandstone
Water Depth	80ft (24m)	Completion Status	P & A

Age	Rock unite	Lithology	Depth
Recent		Water / Sand / Claystone / Limestone	Surface to 1008 f
Pliocene	Zaafarana	Anhydrite / Claystone / Limestone	1008-1165 ft
	Wardan	Sand / Limestone / Claystone	1165-1343 ft
Late Miocene	Zeit/South Gharib	Sand / Shale / Anhydrite / Limestone	1343-2370 f
Middle Miocene	Belayim	Dolomite / Shale / Sand	2370-3409 f
Late Cretaceous (Cenomanian)	Raha	Limestone / Shale / Sand	3409-3932 ft
Early Cretaceous /	Nubian Sandstone	Sand / Shale with Coal	3932-5000 ft

Fig. 2: Composite well log of EWA-1X

3. Surface structures

According to [42] description, Wadi Araba lies along the axis of a broad, gentle, plunging anticlinal structure which has been denuded, where the Northern and Southern Galala plateau (flanks) dip in opposite directions (NW and SE respectively). The axis of this great structure trends NNE-SSW and plunges gently to the southwest. Westwards, this axis rotates from the NE to the NW direction. The effect of topography and the relatively intense down-faulting of the flanks (especially the Southern Galala) minimize the amount of the original uplifting of the anticlinal structure and render it somewhat asymmetrical.

A structural analysis was carried out considering two essential trends in the study area namely African and Clysmic [42]. The Carboniferous rocks exposed in Wadi Araba structure on both sides of its folding axis are highly affected by the two essential faulting trends especially the African trend. Two major faults of the same trend (i.e., African; ENE trending) shown in the geologic map (**Fig. 4**), dislocate these rocks (Upper Paleozoic) from the Cretaceous-Eocene sequences of the Northern and Southern Galala. Also, they are bounded to the east and west by two major Clysmic faults (i.e., NNW trending) with northeastern and southwestern throws. The Pan-African Orogeny raised the southern Sinai and the northern Eastern Desert along a high angle, right lateral thrust-and-shear zone [14]. The structural setting of the region lying to the south of the area under study was investigated by [32] between latitudes 28°00' and 28°30'. He classified (NNE-SSW, NE-SW, NNW-SSE) joint sets and (NE-SW, N-S, NW-SE) fault trends as the three main joint sets and three dominating fault trends affecting the region's varied rock exposures. The surface structures map of the area of Wadi Hawashiya at the southern side of Wadi Araba area was interpreted by [24]. They postulated that the map delineates that the EN-E, NW, N-S and E-W are the dominant trends.

Fig. 4 shows the detailed structure lineaments of the area under study. The visual examination of the detailed surface map shows that the NW-SE, NE-SW, E-W and N-S are the dominant trends recorded in the studied area. These trends are consistent with the subsurface structures and compatible with the adjacent areas.

4. Previous work

The aeromagnetic data acquired in 1981 was analyzed by [22] and studied the Zaafarana accommodation zone, which is adjacent to the study area. He concluded that the Zaafarana accommodation zone cuts across the northern Gulf as a broad EW-trending plateau. The plateau dips westward, and its depth is interpreted to increase from (2,500–3,500) m to (4,500–5,500) m. Aeromagnetic and geoelectric data of the north Al-Ain El-Sokhna area were used by [8], which lies just above the north of the study area, to evaluate the groundwater accumulations in the northwest Gulf of Suez. The results of magnetic interpretation indicated that the mentioned area is dissected by fault elements of N-S and NE-SW. The depth of the basement ranges from 1925–1998 m. The authors [6] carried out an integrated magnetic and stratigraphic study to delineate the subsurface features in and around the New Galala City, Northern Galala Plateau. They deduced that the source depths range from 500 m to 4000 m, which results from the Precambrian basement complex. The trends of encountered structural elements are mainly NE–SW, NW–SE, NNW–SSE and E–W directions. By utilizing gravity, magnetics, and drill holes, the region along the western Gulf of Suez coast was investigated by [11].
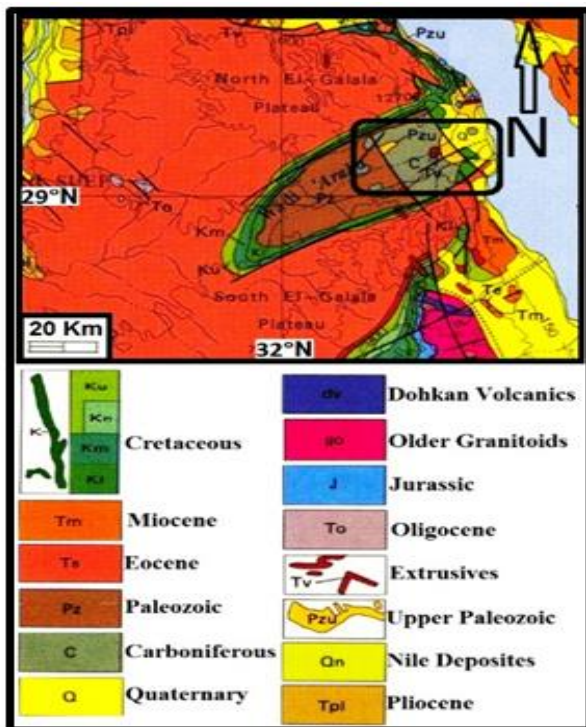
Fig. 3: Map illustrating the study area's geological interpretation [13]; the black box refers to the study area.

They concluded that large horsts and grabens are formed by the regional structure of the study area, especially along a NE-SW direction, perpendicular to the general trend pattern of the fault systems. Additionally, they determined the typical depth up in the basement complex, which was roughly 3000 meters.

The subsurface structural regime of Wadi Araba area was studied by [33] which is located between latitudes 28°50 'N and 29° 15 'N, and longitudes 32° 10 E and 31°40 'E through the qualitative and quantitative interpretation of the available gravity and magnetic data. He concluded that the subsurface structure in the Wadi Araba area is mainly due to block faulting phenomena of the basement complex. He deduced that the depth to the basement ranges from 1 to 1.5 km with an average value of 1.25 Km. [15, 16, 33], reported that the fault systems revealed two prominent trends, namely Suez" NW-SE" and Aqaba "NE-SW" trends. They proposed that the Suez trend is more predominant "and, probably, older than the Aqaba trend". These results match the present work's results. Here we suggested the second trend (NE-SW) is due to the influence of the Syrian arc movement, which appeared mostly in the western part, while the Suez orientation prevailed in the eastern parts of all the analytical maps of the study area; hence, the Syrian arc trend will be older than that of the Gulf of Suez.

According to [17], the Wadi Arab area could be mainly divided into two distinct parts: a southwestern part, which is relatively more deeper (ranging in the calculated depths from 1.736 km to 4.281 km and averaging 3.200 km) and a north-eastern one (where the study area is), which is relatively shallower (ranging in depths from 0.415 km to 4.167 km and averaging 1.800 km). The magnetic data collected over the Gulf

of Suez area was analyzed by [29] to detect the tectonic trends, that govern the region's structural makeup. The study identified five tectonic trends (N85°E, N65°E, N35°E, N65°W and N35°W). The northern compressive force is thought to be the cause of the N35°E and N35°W inclinations. The Red Sea opening-related local tectonic forces are thought to be the cause of the N65°W trend. The aeromagnetic data of the area of Wadi Hawashiya was interpreted by [24] which is adjacent to the Wadi Araba area. The depth estimates calculated for the major magnetic anomalies range between 0.5 and 3.9 km. They traced four main tectonic trends from the total aeromagnetic and shading relief maps. These trends were defined as N60E, N45W and E-W. [41] described Wadi araba structure as a seemingly anticlinal fold consisting of flexure blocks. These are due to the "antithetic faults" Such type of folding was described in Wadi Araba and designated" Tethyan folds" by [27]. [31] referred that the minor domal uplifts encountered in many places in Wadi Araba are synchronous with the great anticlinal arch which embraced the whole of the Gulf of Suez area during the early Oligocene - early Miocene times (Syrian arc). [2] stated that although the wadi Araba structure can be looked at as a large faulted upthrown block (Scholle), however, it is noted that the Carboniferous rocks exposed in its core show that they suffered folding movements. [1] stated that there are minor anticlines and synclines are recognized in Wadi Araba particularly in the Paleozoic rocks of the Rod El-Hamal locality, East Wadi Araba.

5. Material and methods

The total magnetic intensity map (TMI) with a scale of 1:50,000 was used to digitize the magnetic data (**Fig. 5**) after being provided by the Egyptian General Petroleum Corporation [25]. A total magnetic intensity of 42425 nT and a contour interval of 2 nT were used in the survey, which was conducted at flight directions of 45/225o and tie 135/315o, with an inclination angle of 39.5o N and a declination angle of 2o E 7. To create the reduced to magnetic pole (RTP) map, the TMI map was used (**Fig. 6**). Maps of the investigated area's residuals and regionals are extracted using the RTP. Several innovative software packages, including Geosoft (4.8), Rock Ware (15), and Surfer (11), were implemented in the processing and definition phases of the geomagnetic data of the investigation area.

5.1 RTP aeromagnetic data

Reduction to the pole is a mathematical technique that has been proposed by a number of authors [10, 35]. Using this technique, the magnetic anomaly that was actually detected is converted into the anomaly that would have been obtained if the magnetization and surrounding field were both vertical, as if the measurements were taken at the magnetic pole. This technique needs knowing of the magnetization's direction, which is frequently taken to be parallel to the ambient field, as it would be if remnant magnetization were either insignificant or parallel to the ambient field. The RTP data was employed for additional investigation techniques that worked in concert to determine the structural setup for the study area's basement.
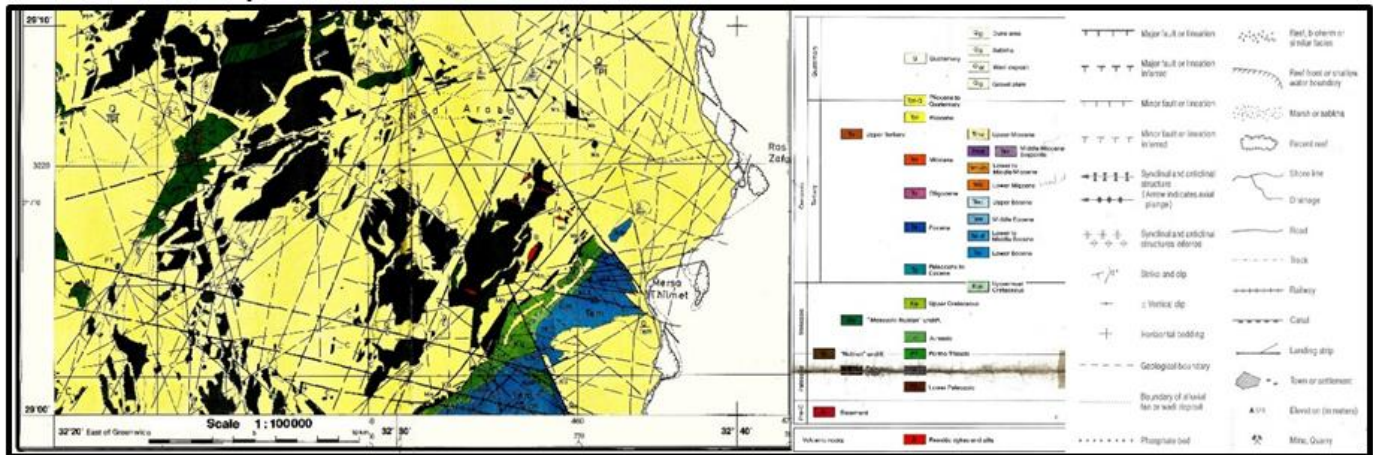
Fig. 4: Detailed interpretation map of the surface structures of Wadi Araba area modified after [12].

5.2. Regional–residual separation

There are many approaches for separating regional and residual magnetic component maps from an RTP map. One of these methods is spectral analysis, which theoretically relies on a fast Fourier transform (FFT). To calculate the energy spectrum curves and determine the regional (deep) and residual (shallow) sources, FFT was implemented to the magnetic data. This filter relies on cut-off frequencies that pass or reject specific frequency values and a specific frequency band [36]. A number of authors described the spectral analysis approach, that relies on the Fourier Transform analysis of magnetic data [36, 44].

5.3. 3D Euler deconvolution

Potential field data was processed according to the 3D Euler deconvolution approach to determine the precise location of the structural lineament. This method does not depend on the source's initial magnetization orientation or how much remanence is present. These techniques calculate gradients, precisely track the edges, and characterize the depth of the source bodies [34].

5.4. Subsurface trends

The two-dimensional trend analysis method was used to quantitatively define the tectonic patterns that had formed in the region. A frequency plot that displays the percentage of trends that fall within certain direction ranges is a common technique for illustrating two-dimensional patterns. A tectonic unit can be identified by its constant magnetic regions [17, 47]. Various patterns are identified for the RTP, the high-pass (residual) and low-pass (regional) filtered magnetic maps, and for two models (contacts and dykes) of the Euler deconvolution solutions of the investigated area. The determined trends' azimuth and length are determined and statistically examined to determine their length and number percentages (L% and N%) as well as the number to length ratios (**Table 1**).

The magnetic lineaments were traced and statistically analyzed in terms of number (N), length (L), L/N ratios, and direction to reveal the basic tectonic trends affecting the area.

The number (N), length (L), L/N ratios of the extracted lineaments are the basic elements of constructing the Rose diagrams. The results of the statistical trend analysis (L%, N%, and L/N ratio) help to detect the number of fractures with a specified cumulative length within the different localities in the study area to determine the predominant orientations and force influences (compressional or tensional) from place to place. L/N ratio refers to the mean distribution of the fault lengths and their throws for the specified orientation.

6. Results and discussion

6.1. The total intensity aeromagnetic map (TMI)

There are several different kinds of positive anomalies (highs) and negative anomalies (lows) seen on the current total intensity aeromagnetic map (**Fig. 5**). However, the map shows that there are significant negative anomalies at the southern half of the mapped area, which is trending WNW-ESE, and strong positive characteristics in circular and elongated forms located at the northern parts of the recorded area. Magnetic anomalies values on the total intensity aeromagnetic magnetic map range from (42194 nT - 42400 nT). While low magnetic anomalies suggest an extensive sedimentary layer in the studied area, high magnetic anomalies imply a thin sedimentary cover in this location. The positive anomalies vary from 42322nT to 42400nT, the negative anomalies vary from 42266nT to 42194 nT, and the intermediate anomalies vary from 42266nT to 42322nT.

6.2. The reduced to magnetic pole map

The total intensity magnetic map used in this work was reduced to magnetic pole RTP, which can be produced automatically using Geosoft Oasis Montaj (2015) utilizing data like declination (2.00°), inclination (39.5°), and field strength(42425 nT).

Applying this technique will move the magnetic anomalies precisely above their actual sources. When comparing the reduced to the magnetic pole map (**Fig. 6**) to the prior total intensity magnetic map (**Fig. 5**), the elimination of the magnetic field's inclination at this location has caused a northward shift in the locations of the inherited magnetic anomalies. The reduced to pole map (**Fig. 6**) displays moderate anomalies between 42250 and 42230 nT and anomalies with magnitudes ranging from 42207 to 42384 nT. Most peaks are still located in the north of the map, particularly on its northwestern and northeastern edges, with two distinct peaks on its southwesterly side. The main trough is still in the center of the map, trending NW-SE parallel to the main Clysmic direction, with an elongation pattern and additional distinct circulation troughs in the southern region.
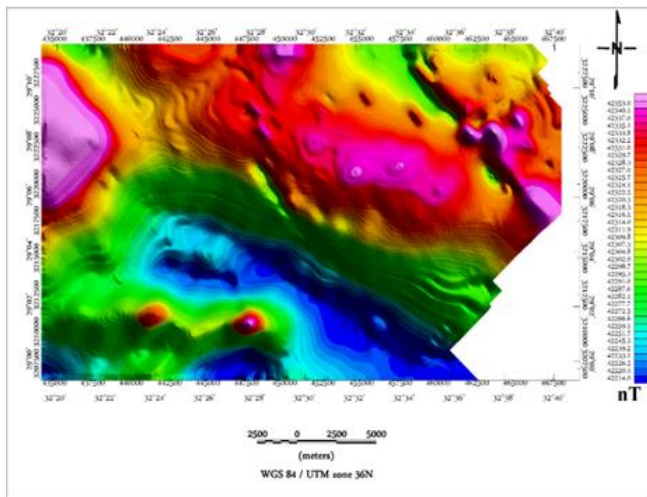

Fig. 5: Aeromagnetic total intensity map of the investigated region.

6.3. The 2D radially averaged power spectrum

Fig. 7 depicts the estimated radially averaged power spectrum of the (RTP) aeromagnetic map. It might be split down into three parts. The first segment, which represents the long wavelengths and is referred to as the regional or deep sources component, has a frequency between 0.00 and 0.01 cycle/km. The second section, which represents the short wavelengths and has a frequency range of 0.01 to 0.03 cycle/km, is known as the residual or shallow sources component. The third segment, at frequencies greater than 0.03 cycle/km, is the noise component. The average depths of the regional and residual magnetic sources are estimated using the slope of lines that correspond to the first and second segments of the spectrum curve, respectively. Regional and residual sources were determined to have estimated mean depths of 2.58 and 1.32 km, respectively. Using the Geosoft Program, the average energy power spectrum for the RTP aeromagnetic data of the investigated area was computed. To determine the typical depths to the top of these deep and shallow sources, use the accompanying depth estimation chart. A low-passes and high-passes map is created based on this diagram.

6.4. High pass filtered map (residuals)

The high pass magnetic map depicts the abrupt variations in magnetic relief that are always present in conjunction with shallow-seated geological structures and/or bodies (**Fig. 8**). It clearly demonstrates a few groups of positive and negative magnetic anomalies with regional variations in both their frequency and magnitude. In most cases, these discrepancies can be attributed to the sources' varying compositions and/or depths. The magnetic anomalies on the high-pass map alternate between being positive and negative, and they can be of different sizes and forms, with magnetic intensities ranging from 23nT to -25nT. In the investigation's area, these anomalies show four main directions, including N-S, E-W, NE-SW, and NW-SE

6.5. Low pass filtered map (regionals)

Deep-seated, high-amplitude magnetic anomalies can be seen on the low pass magnetic map (**Fig. 9**). A close inspection of this map reveals that several of the magnetic anomalies that were shown on the original RTP magnetic map (**Fig. 6**) are still there, although at reduced frequencies and amplitudes. The key trends impacting the entrenched structures of the studied area are highlighted by this regional RTP magnetic map. Along with the NNE-SSW and NNW-SSE trend, which are fewer major trends, these structures almost exclusively have the N-S, NW-SE, and NE-SW structural patterns as their principal trends. Between 42380 and 42210, the low-pass magnetic field can be detected. The principal trough of the investigated area, which follows the NW-SE trend of the Gulf of Suez, is created by a regional decline from the nonwestern and northeastern regions towards the middle of the map. There is a noteworthy negative rounded anomaly that is going north to south on the southern part.

Positive anomalies typically occur in the northwest and northeast, with gentle gradients and wide areal extensions, essentially following the Tethyan or Mediterranean E-W trend. Negative anomalies, which are evenly distributed throughout the research area, are defined as thicker sedimentary rocks enclosed within the fault-bounded borders and displaying isolated basinal structuring. On the contour maps, significant faults can be identified as a string of closed lows. The entire research area, in general, showed residual anomalies that were both positive and negative, indicating a succession of magnetic highs and lows.

6.6 3D Euler deconvolution

To apply the 3D Euler deconvolution approach to the gridded magnetic data that describe contacts, structural index 0.5 was chosen. The RTP aeromagnetic data of Wadi Araba are used in this work to use the usual 3D-ED approach. The window size is 15x15 (grid cell size = 300 m), with a maximum depth tolerance of 15% and a grid interval of 100 m. The map with SI = 0.5 displays a very good grouping of symbols in linear and curved styles, showing the nature of likely interactions between different rock units (**Fig. 10**). As we can see, the solutions are neatly grouped into linear shapes, which leads to complexity in orientations. In the eastern half of the map, especially, the NW-SE (Suez) tendency is dominating.

Another set of trends are noticeable in the region, particularly in the western and southern portions, such as the

NE-SW (Syrian), E-W (Tethyan), and N-S (East-African). These linear solutions implied dykes and fault-controlled contacts. We can observe that shallow sources with depths ranging <1000 m are estimated in the eastern and western portions of the research region.

On the other hand, the western and central portions of the study area have either shallow or deeply seated sources.
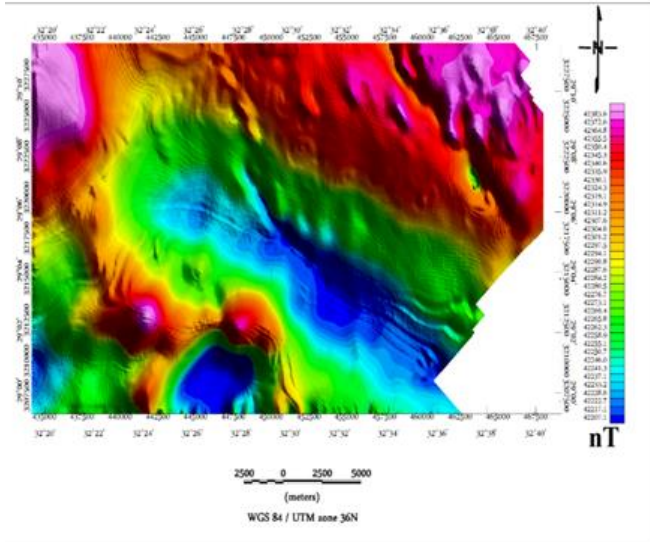

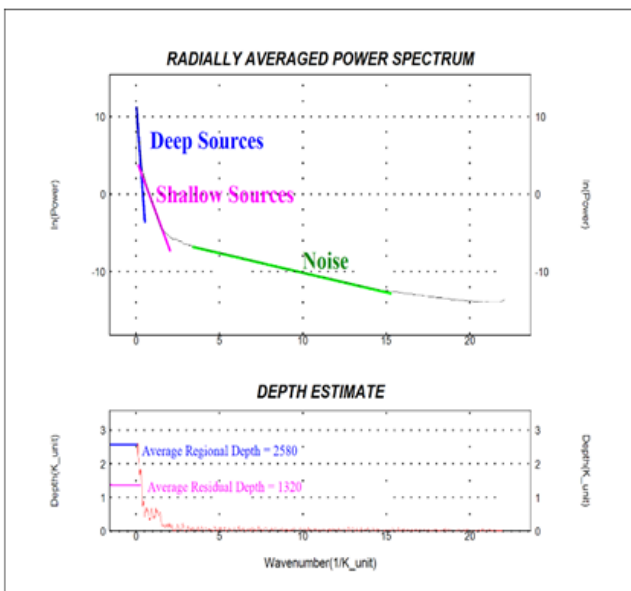**Fig. 6:** Reduced to pole magnetic map of the investigation area.

Fig. 7: Calculated radially averaged power spectrum of the RTP magnetic map.

6.7 Subsurface structures delineation

Fig. 11 displays traced lineaments from the reduced-to-pole magnetic map of the research area. The predominant trend of the obtained lineaments is almost parallel to the Gulf of Suez opening (NW-SE), as shown by the rose diagram (**Fig. 12**) (azimuth frequency), with other notable major trends, such as N-S and E-W, organized accordingly to their
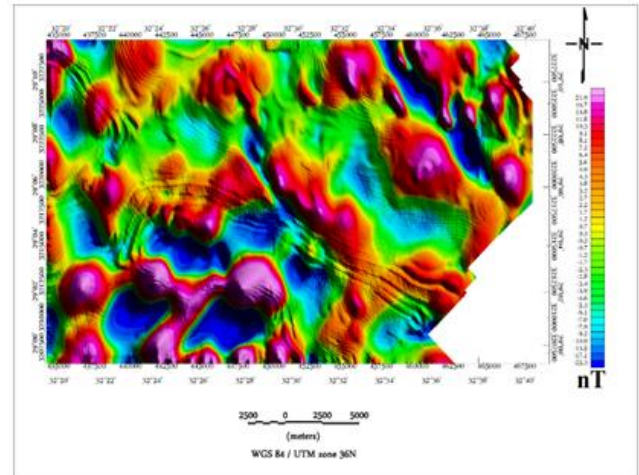
magnitude after the Clysmic trend.

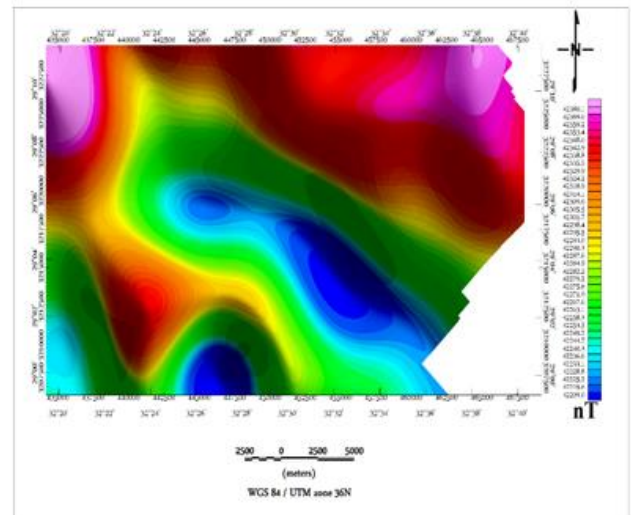**Fig. 8:** High pass filtered map of the study area.

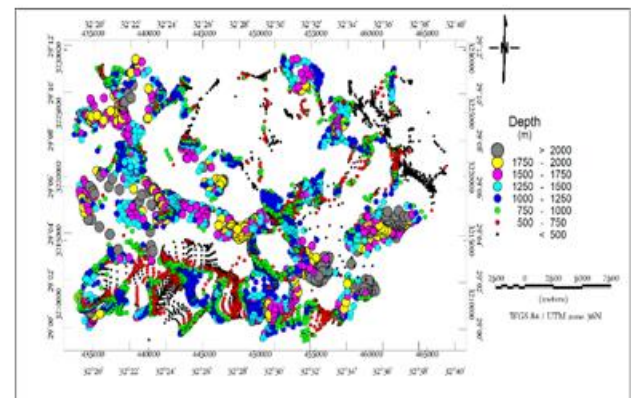**Fig. 9:** Low pass filtered map of the study area.

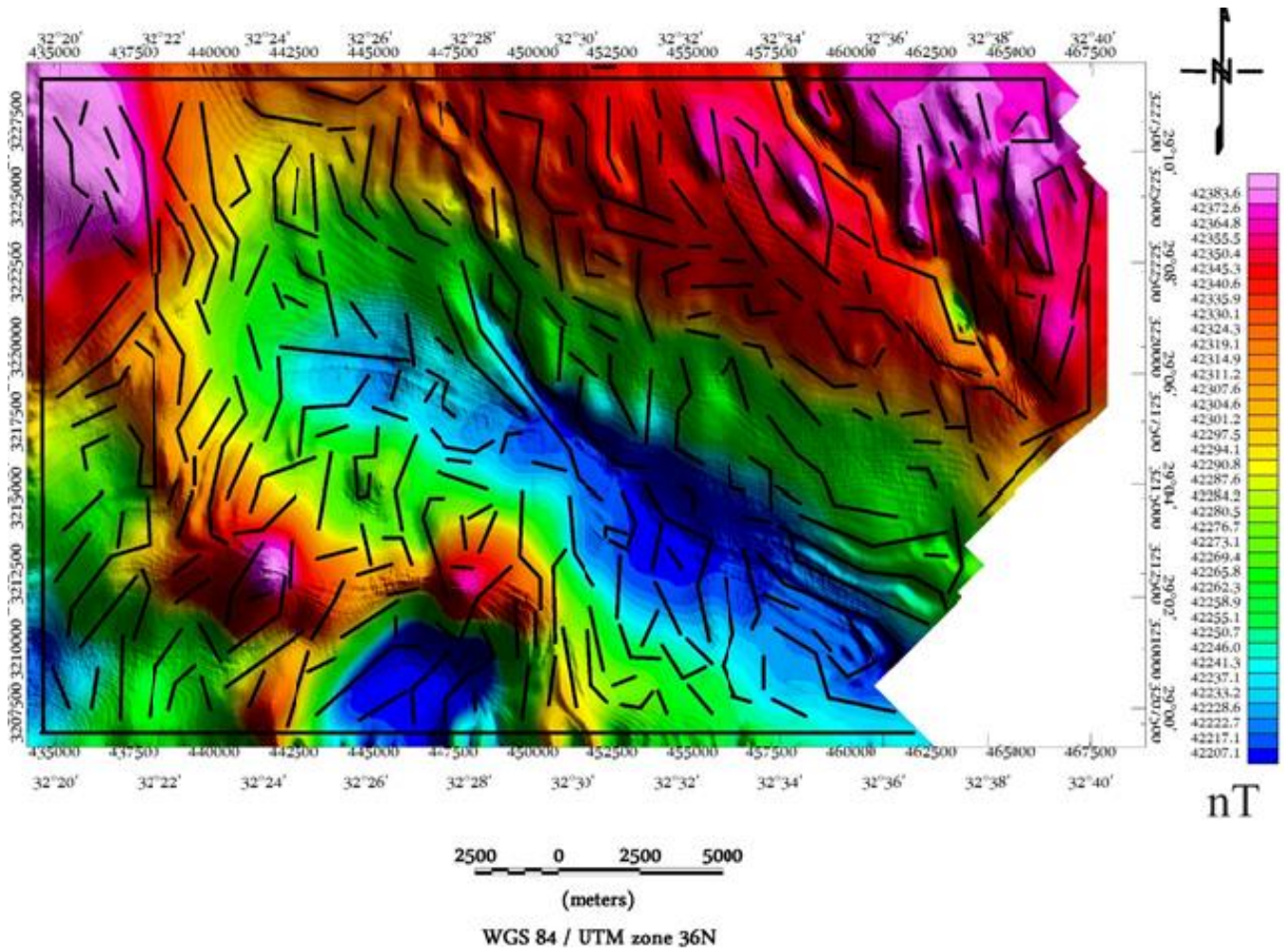**Fig. 10:** 3D Euler contact model (SI=0.5) of the study area

Fig. 11: Lineaments traced from RTP.

Table 1. Features of the main trends identified via the RTP magnetic map. The total number of the traced lineaments is ($\sum$N= 419) and the total lengths of the lineaments is ($\sum$L=542852.35m) where, $\sum$N%=100% and $\sum$L%=100%.

| West					Azimuth	East				
L%	N%	L	N	L/N		L/N	N	L	N%	L%
15%	13%	80481.11	54	1490.39	>00°-10°	1517.59	37	56150.93	9%	10%
11%	10%	58005.23	40	1450.13	>10°-20°	1221.37	20	24427.46	5%	4%
10%	11%	54733.63	46	1189.86	>20°-30°	1201.53	16	19224.51	4%	4%
7%	7%	39296.11	29	1355.04	>30°-40°	1310.36	18	23586.41	4%	4%
4%	5%	22632.07	20	1131.60	>40°-50°	1569.69	10	15696.9	2%	3%
4%	5%	20188.55	20	1009.43	>50°-60°	1492.49	10	14924.93	2%	3%
6%	5%	32029.35	23	1392.58	>60°-70°	1032.78	11	11360.62	3%	2%
3%	4%	18077.12	17	1063.36	>70°-80°	1089.54	10	10895.44	2%	2%
4%	5%	21061.11	21	1002.91	>80°-90°	1181.23	17	20080.87	4%	4%
64%	64%	346,504	270		Total		149	196,348	36%	36%
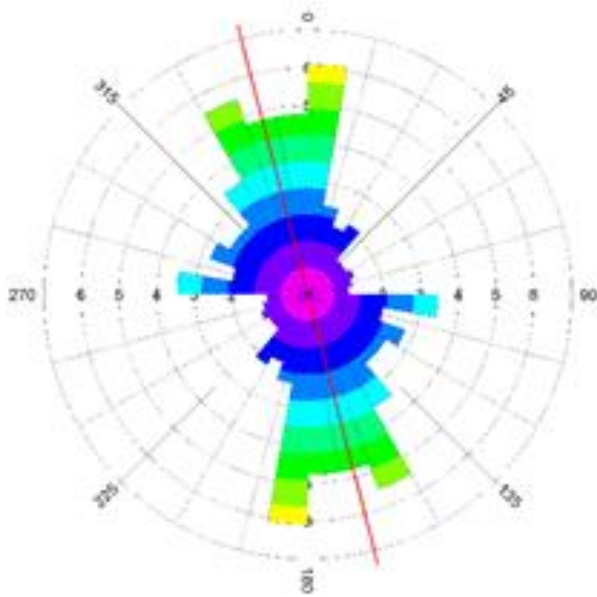
Fig. 12: Rose diagram of the traced lineaments from the RTP.

Conclusion

Aeromagnetic map was utilized to identify the underlying features of wadi Araba area which associated to the petroleum traps. From the several used maps and methods at various horizons of depth; the study area could be represented by a series of horsts (domes or anticlines) and grabens (troughs, basins or synclines). The results of all methods of depth determination and trend analysis suggest a fault-controlled structural regime. Qualitative and quantitative trend analysis was carried on the RTP, high pass, low-pass, Euler (SI=0.5) resulted in four major trends in the study area, NW-SE (Suez Rift), NE-SE (Syrian Arc), E-W (Tethyan) and N-S (East African) arranged in decreasing order of frequency magnitude where, the trends of Suez and the Syrian are the most prevailing. The Suez orientation prevailed in the eastern parts, while the Syrian Arc trends appeared mostly in the western part of the studied area. Using the 2D power spectrum and 3D Euler deconvolution techniques, depth estimation is carried out. EWA-1X well reached the Nubian Sandstones at total depth 1524 m (5000 ft). The estimated depth to the basement complex is between 0.5 and 3 km, average 1.8 km. EWA-1X composite well log (**Fig. 2**) is used (with the available previous studies) to correlate the deduced results which are compatible with these studies and the well data.

Acknowledgments

References

[1] M.I. Youssef, *AAPG Bulletin* 52 (1968) 601-614.

[2] W.M. Meshref, E.M. Refai, and S. Abdel-Baki. *EGPC 5th Exploration Seminar, Cairo, Egypt*. 1976.

[3] S. Riad, Geophysics 6 (1977) 1207-1214.

[4] H.A. Eletr, M.A. Abdel-Rahman, Egypt Proc. Egypt. Acad. Sci., 26 (1973) 37-44.

[5] S.W. Tromp, *Block folding phenomena in the Middle East.* Geologie en Mijnbouw 11 (1949) 273-278.

[6] F. Heybroek, *Geological Society Circular* 121 (1965) 3-4.

[7] M.S. Garson, M. Krs, *Geological Society of America Bulletin* 87 (1976) 169-181.

[8] S. Nakkady, Bull. Inst. Egypt 36 (1955) 254-268.

[9] F. Irving, *Report on a Detailed Reconnaissance of Wadi Araba (Gulf of Suez, West Coast).* Unpublished report of AEOC, 1945.

]10] K. Bandel, J. Kuss, *Berliner geowiss.Abh. A* 78 (1987) 1-48.

[11] J. Shahar, *Palaeogeogr. Palaeoclimatol. Palaeoecol.* 112 (1994) 125-142.

[12] A.A. Abdel Monem, M.A. Heikal, Fac. Earth Sci. Bull., King Abdul Aziz Univ., 4 (1981) 121-148.

[13] A.M. Abdallah, M.Y. Meneisy, and M.M. Shaaban, *Eg. J. Geo.* 1973. **17**(2): p. 111-123.

[14] A.M. Abdallah, *Geological Survey and Mineral Resource Department*, Egypt, 25 (1963) 18.

[15] M.A. El-Sadek, A. Ammar, A. Sabry, *Arabian Journal for Sci. and Eng.,* 27 (2002) 131-148.

[16] H. Sadek, *Geological Survey and Mineral Resource Department* 40 (1926)120.

[17] A.M. Abdallah, A. Adindani and N. Fahmy, *Geological Survey and Mining Resources Department* 27 (1963) 23.

[18] M. Wilmsen, E. Nagm, Facies 58 (2012) 229-247.

[19] E.M. El-Shazly, Nucl. Mater. Energy 1977, Unpublished Report, (NMA), Egypt.

[20] R. Said, *Eg. J. Geo.* (1990) 734. Balkema, Rotterdam.

[21] E.M. El-Shazly, Annals of the Geological Survey of Egypt 9 (1979) 551-563.

[22] R. Said, , *The geology of Egypt*. 2017: Routledge.

[23] M.M. Shabaan, Fac. Sci. 1971.

[24] S. El-Gaby, *Proceeding of the Fifth International Conference on Basement Tectonics, Cairo* (1983) 1-8.

[25] L.M. Nossair, , *D.J. Sci.*, 20 (1996) 65-91.

[26] H.I. Hassanein, K.S. Soliman, *Egypt. J. KAU: Earth Sci.*, 20 (2009) 117-139.

[27] EGESMA, E.G.S.a.M.A., Egyptian Geological Survey and Mining Authority (1981).

[28] K.Farhoud, *Geo.Arabia*., 14 (2009) 139-162.

[29] S.A.S. Araffa, H. Saleh Sabet and M.A. Abed, *NRIAG J. Astron. Geophys.,* 9 (2020) 280-288.

[30] M. Abdelazim, et al., *NRIAG J. Astron. Geophy.,* 5 (2016) 393-402.

[31] A. Bayoumi, J. Boctor, *UAR 7th Arab Pet.* Con. *Secret. Gen. Leag*. Arab State, Kuwait, 1970. **2**: p. 36.

[32] M.A. El-Sadek, PhD Thesis *Fac. of Sc.,* Ain Shams Univ., (1998) 320 p.

[33] W.M. Meshref, and M.M. El-Sheikh, Eg. J. Geol., 17 (1973) 179-184.

[34] R. Said, *The Geology of Egypt.* 1962, New York: Elsvier.

[35] W.F. Hume, *The Geology of Egypt: A Digest of Papers Published on Egypt*. 1925: Government Press.

[36] M. Hayatudeen, , et al., J. pure appl. sci., 27 (2021) 181-192.

[37]   Aero-Service, *The Egyptian General Petroleum Corporation (EGPC) and the Egyptian Geological Survey and Mining Authority (EGSMA)*, 1984, Aero-Service Division Houston,Texas.: Houston, Western Geophysical Co., Taxas, USA.

[38] V. Baranov Geophysics, 22 (1957) 359-382.

[39] M. Rajaram, Geohorizons, (2009) 50.

[40]   Conoco, *Photogeological Interpretation Map*, 1983, Conoco Coral INC., : Cairo, A.R.E.

[41] A.B. Reid, et al., Geophysics, 55 (1990) 80-91.

[42] J.B. Thurston, and R.S. Smith, 62 (1997) 807-813.

[43] N.R. Paterson, C.V. Reeves, Geophysics, 50 (1985) 2558-2594.

.